

The nextSENSE system: Short-term forecasting of solar energy in Europe and North Africa

Kosmopoulos P.G.^{1,2*}, Kazadzis S.^{3,1}, Kouroutsidis D.², Papachristopoulou K.^{2,4}, Saint-Drenan Y.M.⁵, Kontoes C.² and Blanc P.⁵

1 Institute for Environmental Research and Sustainable Development, National Observatory of Athens(IERSD/NOA), Greece

2 Institute for Astronomy, Astrophysics, Space Applications and Remote Sensing, National Observatory of Athens (IAASARS/NOA), Greece

3 Physikalisch Meteorologisches Observatorium Davos, World Radiation Center (PMOD/WRC), Switzerland

4 Department of Geology and Geoenvironment, National and Kapodistrian University of Athens, Greece

5 MINES ParisTech, PSL Research University, O.I.E. Centre Observation, Impacts, Energy, SophiaAntipolis, France

*corresponding author e-mail: pkosmo@noa.gr

Abstract: In the framework of the EuroGEO e-shape project (<http://www.e-shape.eu/>) we introduce the pilot system nextSENSE, which is capable of short-term forecasting the surface solar radiation (SSR) and the subsequent energy production by the photovoltaic solar power plants in Europe and North Africa. This system was developed by the National Observatory of Athens in Greece in collaboration with the World Radiation Center of Davos in Switzerland and uses Earth observations from the satellite application facilities to support nowcasting and very short range forecasting (SAFNWC) of the European organization for the exploitation of meteorological satellites (EUMETSAT) and the Copernicus Atmosphere Monitoring Service (CAMS). The algorithmic part of the nextSENSE system consists of state-of-the-art fast radiative transfer models (FRTM) powered by high performance computing (HPC) architectures and computer vision aspects in order to short-term forecast the clouds motion and the impact on solar energy. The outcome is a massive provision (i.e. 20 million simulations per minute for Europe and North Africa) of operationally produced solar energy simulations in 5 km spatial resolution for a forecast horizon of 3 hours ahead in 15-minute time intervals in real-time. NextSENSE is going to support the solar energy producers and the local and regional electricity handling entities.

1 Introduction

The renewable energy market requires an efficient and optimal energy planning and management. The modern technical solutions for the grid operators support monitoring, forecasting, and managing the energy production with the use of space technologies, which are in particular useful in decision-making for the energy producers that exploit photovoltaic or concentrated solar power plants as well as for the electricity transmission and distribution system operators. To this direction, in the framework of the EuroGEO e-shape project a novel system was officially released in summer 2020 in support to the distributed solar plant energy production management, electricity handling entities and smart grid operations in Europe and North Africa. Called NextSENSE, this system is a 5-year scientific and technical achievement of the collaboration of the National Observatory of Athens (NOA) in Greece with the World Radiation Center (PMOD/WRC) in Switzerland and exploits the synergy of Earth observation (EO) data and radiative transfer modeling with image processing, optical flow technologies and HPC architectures.

2 Data and Methodology

2.1 Data

The main Earth Observation data source used as input the nextSENSE is the cloud optical thickness (COT) product of the EUMETSAT's SAFNWC, retrieved from the Meteosat Second Generation SEVIRI instrument (MSG/SEVIRI), in near-real time (nowcasting). The retrieval algorithm uses radiances from the 0.6 and 1.6 micron channels (MétéoFrance 2013). The spatial and temporal resolution of the MSG COT is 5 km over nadir and 15 minutes respectively, indicating also the moving step for the short-term forecasting techniques. For the calculation of the clouds effect on SSR we used the Cloud Modification Factor (CMF) for more generalized results and for better understanding of the overall impact regardless the climatological conditions. The CMF is described as:

$$CMF = SSR / SSR_{cls}, \quad (1)$$

where SSR is the irradiance under actual sky conditions and SSR_{cls} is the irradiance under clear sky conditions as simulated by the FRTM. As a result, the CMF takes values between 0 and 1, indicating the clear sky SSR with 1 (i.e. no cloud effect) and all the lower values characterizing the SSR under the clouds effect. For the aerosol effect on SSR (Kosmopoulos et al. 2017) and solar energy production (Kosmopoulos et al. 2019) the aerosol optical depth (AOD) 1 day fore-

casts from the CAMS service was used operationally at 1 hour and 40 km temporal and spatial resolution, respectively.

2.2 Methodology

For the short-term forecasting dimension of the nextSENSE system, we obtain cloud motion vectors (CMV) in order to predict the motion of the clouds by applying computer vision techniques and particularly calculating the optical flow displacement vectors between two images of satellite derived cloud related parameters, COT and CMF, by assuming that cloud's displacements are two dimensional (image plane). The problem of optical flow estimation can be outlined as the approximation of the motion field from image intensity variations with time, solely attributed to objects displacement, so the image intensity $I(x, y, t)$ satisfies the following equation:

$$I(x, y, t) = I(x + dx, y + dy, t + dt) \quad (2)$$

where for an infinitesimal time interval dt , dx and dy are the horizontal and vertical displacements of an image region (pixel). The innovation relies on the implementation of a state-of-the-art method of computer vision (Farnebäck 2003), which is a two-frame motion estimation technique based on polynomial expansion in the neighborhood of each pixel, and then to calculate the optical flow using satellite images, in order to calculate CMVs and forecasting cloudiness (Kosmopoulos et al. 2020). We benchmarked the CMV against the persistence (PeRsiStence; PRS hereafter) approach which assumes that clouds remain motionless for the next 3 hours, while all the other parameters change dynamically including the solar zenith angle, the aerosol impact etc.

The nextSENSE system exploits the FRTM described in Kosmopoulos et al. (2018) which is based on large scale pre-calculated look up tables (i.e. 2.5 million simulations using the libRadtran library of RTM (Mayer and Kylling 2005)), the CMV method described in Kosmopoulos et al. (2020) in conjunction with the aforementioned Earth Observation data sources and HPC in order to work operationally and in real-time. Figure 1 illustrates the operation of nextSENSE, the input data sources (MSG COT and CAMS AOD) and the subsequent output results in the form of an open access web service (<http://solea.gr/solar-energy-management/>) developed in the framework of the EuroGEO e-shape project. The user through the fully dynamical interface is able to navigate, zoom and click at any pixel of the 1.5 million matrix retrieving solar energy potential information for 3 hours ahead and 3 hours back time horizons at 15-min intervals. For the almost 20 million RTM simulations required every 15 minutes (1 matrix of 1.5 million pixels for the current time and 12 matrixes of 1.5 million pixels for the 3 hours ahead time horizon, i.e. 12 time steps), a distributed and HPC was exploited at a UNIX featured environment. For this purpose, a 32-core independent core architecture is used followed by a 256 Gb RAM, distributed into 16 virtual machines working in parallel and in real time. The daily dataflow including the input and output data retrieving, production and projection is of the order to 550Gb handled by a 12Tb RAID10 storage architecture.

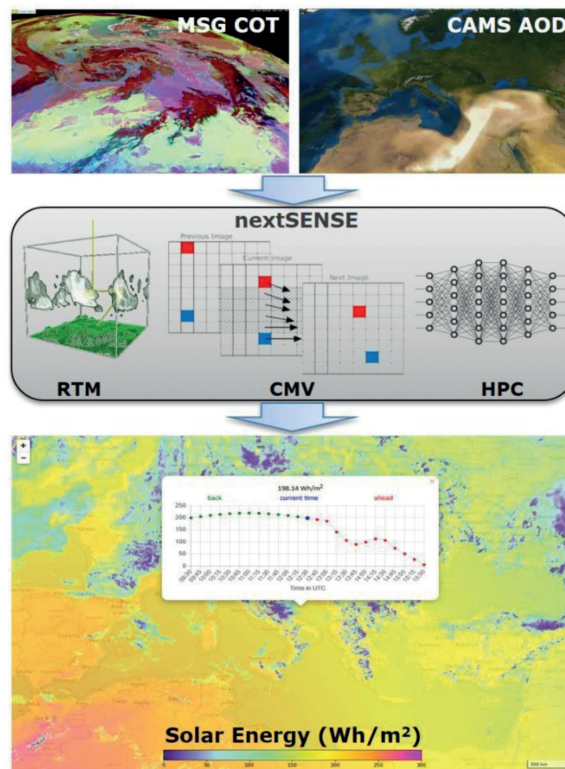


Fig. 1. Flowchart illustration of the nextSENSE system.

The forecasting results are evaluated in terms of mean bias and root mean square error (MBE and RMSE, respectively), defined in absolute terms as follows:

$$MBE = \bar{\varepsilon} = \frac{1}{N} \sum_{i=1}^N \varepsilon_i \quad (3)$$

$$RMSE = \sqrt{\frac{1}{N} \sum_{i=1}^N \varepsilon_i^2} \quad (4)$$

Where $\varepsilon_i = x_f - x_0$ are the residuals calculated as the difference between the forecasted values (x_f) and the real observed values (x_0), and N is the total number of values. RMSE describes the overall spread of the error distribution, while MBE quantifies the bias and additionally detects overestimations ($MBE > 0$) or underestimations ($MBE < 0$). Finally, the correlation coefficient (R), as well as the standard deviation (SD) were used to represent the proportion of the variability between the forecasted and real observed values.

Results

Figure 2 shows for the 30th of April 2020 the differences between the forecasted CMF (i.e. the CMV CMF) and the real CMF for 3 hours ahead at the left map and at the right map the same for the PRS. Both maps present positive and negative differences indicating the subsequent overestimation and underestimation of the CMV and PRS approaches, respectively. The PRS results larger errors both as underestimation and as overestimation than the CMV as indicated by the more intense red and blue areas on the maps, highlighting the limited ability of the PRS to follow the cloud movement and the corresponding impact on the CMF.

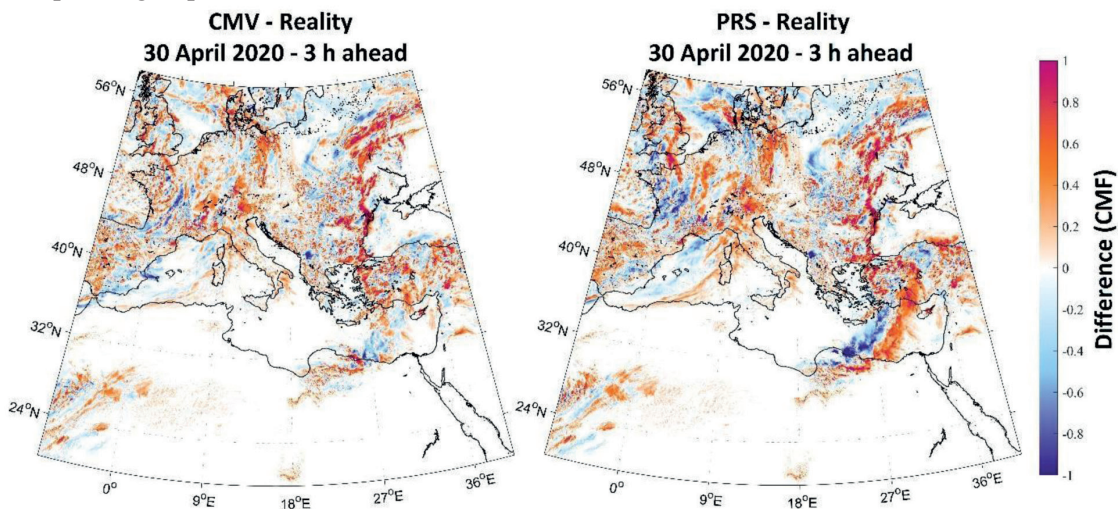


Fig. 2. Difference between the CMV and the real CMF (left plot) during the 30th of April 2020 at 3 hours ahead time horizon, as well as the difference between the PRS and the real CMF (right plot) for the same time horizon.

Figure 3 shows, for the same day (30th of April 2020), the density scatter plots for the CMV forecasted (left plot) and PRS (right plot) approaches in terms of CMF, for 15min ahead, against the real retrievals.

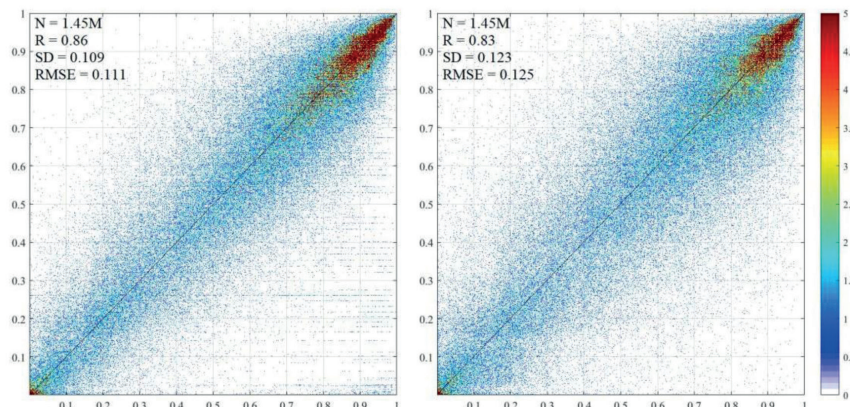


Fig. 3. Density scatter plots of the 30th of April 2020 covering Europe and North Africa (i.e. 1.5 million pixels) for the CMV (left plot) and PRS (right plot) short-term forecast approaches for the 15-min ahead time horizon.

The PRS method presents a larger scatter in comparison to the CMV approach followed by the corresponding statistics, i.e. $R=0.83$, $SD=0.123$ and $RMSE=0.125$ for the PRS and $R=0.86$, $SD=0.109$ and $RMSE=0.111$ for the CMV, respectively. This is a result of the changing clouds conditions, which by definition PRS cannot forecast.

Figure 4 presents the overall CMF error as a function of RMSE and MBE for PRS and CMV approaches under all conditions and during transition. A note for this kind of analysis is that the PRS in some cases, like going from cloudy to clear sky conditions, presents better results than starting from clear sky to cloudy sky because returning to clear sky or CMF equals to 1 means that we go back to the optimum operating conditions for PRS, which are the clear sky conditions. So, taking into account that for the studied region, which has almost 1.5 million pixels, the majority is clear sky, around 700 to 800 thousand pixels, it is obvious that persistence is the prevailing situation that will have the best statistics. And this is the main reason that in this plot focuses on the sky conditions changes and the transition (TRN) between clear and cloudy sky.

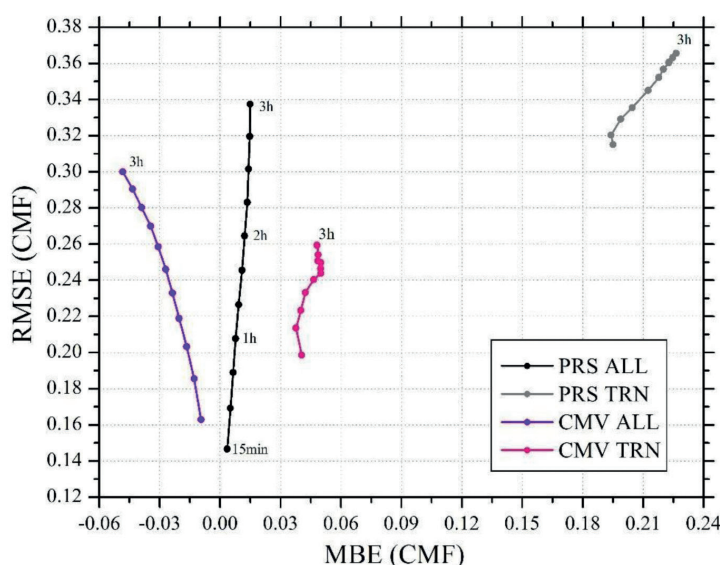


Fig. 4. The overall CMF error for CMV and PRS approaches under all and transition (TRN) conditions as a function of RMSE and MBE.

Under all conditions for PRS, MBE is observed to be almost constant but RMSE is increasing from 0.14 to 0.34 at 15 min and 3 h forecast horizons, respectively which suggests that the distribution is moving from evenly distributed error to large error outliers. The CMV is showing a negative relation between RMSE and MBE which indicates underestimations of CMF under ALL condition. In TRN regime, PRS shows an almost linear increase in RMSE with MBE from 15 min to 3 h forecast horizon, while CMV shows an increase in RMSE though the MBE remains almost constant at 0.05 with very minute deviations. The limited ability of the PRS method was revealed during the TRNs. Indicatively, the highest RMSE of the CMV TRN which is at the 3h ahead time horizon is almost 0.06 CMF lower than the starting point of the PRS TRN at the 15 min ahead (i.e. 0.32), highlighting the overall value of the CMV against the PRS.

4 Conclusions

The nextSENSE system, exploiting the modern Earth Observation (satellite and modelled data) and computer vision (motion flow) technologies is able to act as an open access platform for continuous monitoring and short-term forecasting of solar energy in large-scale, running operationally, online and in real-time. The brief analysis performed in this study revealed the superiority of the CMV method against the PRS under all sky conditions and especially under TRS conditions. The correlation between the forecasted and the actual data was seen to deteriorate with the increasing forecast horizon (from 15 min to 3 h). This system currently provides access to solar energy information mainly for intraday energy management and grid stability, while it can actively support the energy producers at any solar system scale as well as the transmission and distribution system operators in Europe, North Africa and recently in Southern Asia (Masoom et al. 2020), promoting and supporting the sustainable development as well as affordable and modern energy for all.

Acknowledgments This research has been partly funded by the European Commission project EuroGEO e-shape (grant agreement No 820852).

References

- Farnebäck G (2003) Two-Frame Motion Estimation Based on Polynomial Expansion. *Lect. Notes Comput. Sci.* 2749:363–370. https://doi.org/10.1007/3-540-45103-X_50.
- IEA (2019) Solar Energy: Mapping the Road Ahead, IEA, Paris. Available online: <https://www.iea.org/reports/solar-energy-mapping-the-road-ahead>.
- Kosmopoulos PG, Kazadzis S, Taylor M, Athanasopoulou E, Speyer O, Raptis PI, Marinou E, Proestakis E, Solomos S, Gerasopoulos E, Amiridis V, Bais AF, Kontoes C (2017) Dust impact on surface solar irradiance assessed with model simulations, satellite observations and ground-based measurements. *Atmos. Meas. Tech.* 10:2435-2453, doi:10.5194/amt-10-2435.
- Kosmopoulos PG, Kazadzis S, Taylor M, Raptis PI, Keramitsoglou I, Kiranoudis C, Bais AF (2018) Assessment of surface solar irradiance derived from real-time modelling techniques and verification with ground-based measurements. *Atmos. Meas. Tech.* 11(2):907–924. doi.org/10.5194/amt-11-907-2018.
- Kosmopoulos PG, Kazadzis S, El-Askary H, Taylor M, Gkikas A, Proestakis E, Kontoes C, El-Khayat MM (2019) Earth-Observation-based estimation and forecasting of particulate matter impact on solar energy in Egypt. *Remote Sens.* 10(12):1870, doi:10.3390/rs10121870.
- Kosmopoulos PG, Kouroutsidis D, Papachristopoulou K, Raptis PI, Masoom A, Saint-Drenan YM, Blanc P, Kontoes C, Kazadzis S (2020) Short-Term Forecasting of Large-Scale Clouds Impact on Downwelling Surface Solar Irradiation. *Energies* 13(24), 6555. <https://doi.org/10.3390/en13246555>.
- Masoom A, Kosmopoulos PG, Bansal A, Kazadzis S (2020) Solar energy estimations in India using remote sensing technologies and validation with sun photometers in urban areas. *Remote Sens.* 12(2):254, doi:10.3390/rs12020254, 2020.
- Mayer B, Kylling A (2005) Technical note: The libRadtran software package for radiative transfer calculations – description and examples of use. *Atmos. Chem. Phys.* 5: 1855–1877, doi:10.1155/2013/852090.
- MétéoFrance (2013) Algorithm theoretical basis document for cloud products (CMa-PGE01 v3.2, CT-PGE02 v2.2 & CTTH-PGE03 v2.2), Technical Report SAF/NWC/CDOP/MFL/SCI/ATBD/01, Paris